10-1-2021

Satellite-detected ammonia changes in the United States: Natural or anthropogenic impacts

Yaqian He
University of Central Arkansas, xuro@oregonstate.edu

Rongting Xu
Oregon State University

Stephen A. Prior
USDA Agricultural Research Service

Di Yang
University of Wyoming

Anni Yang
Colorado State University

See next page for additional authors

Authors
Yaqian He, Rongting Xu, Stephen A. Prior, Di Yang, Anni Yang, and Jian Chen

Science of the Total Environment 789 (2021) 147899

Contents lists available at ScienceDirect

Science of the Total Environment

journal homepage: www.elsevier.com/locate/scitotenv

Satellite-detected ammonia changes in the United States: Natural or anthropogenic impacts

Yaqian He [a,1], Rongting Xu [b,*,1], Stephen A. Prior [c], Di Yang [d], Anni Yang [e,f], Jian Chen [g]

[a] Department of Geography, University of Central Arkansas, Conway, AR, USA
[b] Forest Ecosystems and Society, Oregon State University, Corvallis, OR, USA
[c] USDA-ARS National Soil Dynamics Laboratory, Auburn, AL, USA
[d] Wyoming Geographic Information Center, University of Wyoming, Laramie, WY, USA
[e] Department of Fish, Wildlife, and Conservation Biology, Colorado State University, Fort Collins, CO, USA
[f] National Wildlife Research Center, United States Department of Agriculture, Animal and Plant Health Inspection Service, Fort Collins, CO, USA
[g] Department of Computer Science and Software Engineering, Samuel Ginn College of Engineering, Auburn University, Auburn, AL, USA

HIGHLIGHTS

- Besides the US Midwest, a striking increase in NH_3 concentrations was also detected in the Mid-South and Western regions.
- Warmer winters in the West and hot summers in the Mid-South and Midwest highly accounted for increased NH_3 emissions there.
- Synthetic N fertilizer interaction with temperature could stimulate NH_3 releases, especially in more vulnerable regions.

GRAPHICAL ABSTRACT

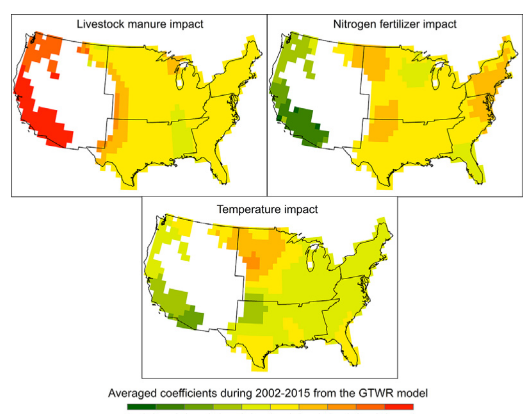

ARTICLE INFO

Article history:
Received 6 March 2021
Received in revised form 6 May 2021
Accepted 17 May 2021
Available online 25 May 2021

Editor: Pingqing Fu

Keywords:
Ammonia
AIRS
GTWR
Synthetic nitrogen fertilizer
Livestock manure
Climate change

ABSTRACT

Ammonia (NH_3) is the most abundant alkaline component and can react with atmospheric acidic species to form aerosols that can lead to numerous environmental and health issues. Increasing atmospheric NH_3 over agricultural regions in the US has been documented. However, spatiotemporal changes of NH_3 concentrations over the entire US are still not thoroughly understood, and the factors that drive these changes remain unknown. Herein, we applied the Atmospheric Infrared Sounder (AIRS) monthly NH_3 dataset to explore spatiotemporal changes in atmospheric NH_3 and the empirical relationships with synthetic N fertilizer application, livestock manure production, and climate factors across the entire US at both regional and pixel levels from 2002 to 2016. We found that, in addition to the US Midwest, the Mid-South and Western regions also experienced striking increases in NH_3 concentrations. NH_3 released from livestock manure during warmer winters contributed to increased annual NH_3 concentrations in the Western US. The influence of temperature on temporal evolution of NH_3 concentrations was associated with synthetic N fertilizer use in the Northern Great Plains. With a strong positive impact of temperature on NH_3 concentrations in the US Midwest, this region could possibly become an atmospheric NH_3 hotspot in the context of future warming. Our study provides an essential scientific basis for US policy makers in developing mitigation strategies for agricultural NH_3 emissions under future climate change scenarios.

* Corresponding author.
E-mail address: xuro@oregonstate.edu (R. Xu).
[1] These authors contributed equally.

https://doi.org/10.1016/j.scitotenv.2021.147899

1. Introduction

Over the last century, the global nitrogen (N) cycle has been heavily perturbed by additions of reactive N from human activities, including combustion-related nitrogen oxides (NO_x), industrial ammonia (NH_3) production through the Haber-Bosch process, and agricultural N fixation (Fowler et al., 2015). These anthropogenic activities have considerably increased atmospheric NO_x and NH_3 (Tian et al., 2020; Xu et al., 2019). Synthetic N fertilizer application and livestock manure management are two dominant atmospheric NH_3 sources that account for ~80% of total NH_3 emission in the US (Davidson et al., 2011). Meanwhile, NH_3 volatilization can be regulated by changing climate. Recent studies have demonstrated that climate warming may favor NH_3 release from multiple surface layers such as soil, stomates, and moisture layers on leaf cuticles (Shen et al., 2020a; Xu et al., 2019). Shen et al. (2020a) projected that climate warming would increase NH_3 emissions by 18% and lead to a considerable drop in crop yield due to a 10% loss of applied N. This could also induce a 14% increase in NH_4^+ deposition to sensitive ecosystems across the US over the 2010 to 2100 time span (Shen et al., 2020a). Increased atmospheric NH_3 can cause a number of environmental issues. NH_3 is the most abundant alkaline component and can neutralize acidic species such as SO_2 and NO_x to form atmospheric aerosols (e.g., $PM_{2.5}$) that can reduce visibility and threaten human health and life expectancy (Bauer et al., 2016; Xu et al., 2018). Moreover, dry and wet depositions of NH_4^+ from NH_3 emissions may alter soil and water chemistry (e.g., eutrophication) and reduce biological diversity (Clark and Tilman, 2008). Thus, better understanding of atmospheric NH_3 magnitudes, trends, and spatial patterns is essential to avoid negative effects on human health and ecosystem function in the US.

Numerous studies have examined changes in spatiotemporal patterns of atmospheric NH_3 concentration (Li et al., 2017; Nair et al., 2019; Van Damme et al., 2020; Van Damme et al., 2018; Warner et al., 2017), agricultural NH_3 emissions (Cao et al., 2020; Shen et al., 2020a; Xu et al., 2018; Xu et al., 2019), and wet NH_4^+ deposition (Du, 2016; Du et al., 2014) over the US using a variety of bottom-up and top-down approaches. For instance, Nair et al. (2019) used a global 3-D chemical transport model (GEOS-Chem) to simulate NH_3 concentration based on surface observations from 90 National Atmospheric Deposition Program Ammonia Monitoring Network (AMoN) sites. They found that NH_3 concentration was highly emission dependent and dominated by agricultural activities, with high NH_3 emissions in the Central US and Western US due to N fertilizer applications and livestock grazing, respectively. A similar conclusion was reached by Van Damme et al. (2018), who found that intensive animal farming can contribute to numerous hotspots of NH_3 emissions across the Western US (e.g., Eckley-Yuma, Colorado; Bakersfield and Tulare, California; and Milford, Utah); this work was based on a high-resolution map of atmospheric ammonia obtained from daily Infrared Atmospheric Sounding Interferometer (IASI) satellite observations over the past decade. In contrast, a recent study on synthetic N fertilizer application identified that increased NH_3 emission hot spots have shifted from the Central US to the Northern Great Plains since 1960 (Cao et al., 2020). Spatiotemporal patterns of NH_4^+ deposition have also been examined. By analyzing 151 site-level annual wet deposition data from the National Atmospheric Deposition Program (NADP), Du et al. (2014) noted that wet NH_4^+ deposition significantly increased over the 1985–2012 period in the Midwest, South, and Western regions of the US. The increased NH_4^+ deposition in the West and Midwest was associated with large animal breeding (e.g., hogs and cattle) and N fertilizer application, while the increase in the Southeast was associated with smaller livestock (e.g., chickens) (Stephen and Aneja, 2008). However, no above-mentioned study has simultaneously considered natural and anthropogenic impacts on decadal spatiotemporal changes in US NH_3 concentrations. Moreover, geographical and temporal weighted regression (GTWR), a unique statistical technique, is capable of accounting for local effects in both space and time (Fotheringham et al., 2015) and has been widely applied in research fields of economics (Qu et al., 2020), transportation (Shen et al., 2020b), infectious disease (Hong et al., 2021), biology (Cullen and Guida, 2021), etc. Our study is a first attempt to examine spatiotemporal influence of climate variability and anthropogenic nitrogen additions on NH_3 concentration dynamics using a GTWR model.

In recent years, satellite-based data have become a promising way to monitor global atmospheric NH_3 due to the relatively high temporal and spatial coverage (Van Damme et al., 2020; Van Damme et al., 2018; Warner et al., 2017). Van Damme et al. (2020) analyzed an 11-year NH_3 dataset (2008 to 2018) obtained from daily IASI satellite observations and found a large increase in atmospheric NH_3 for the US that was highly concentrated in the Midwest. Using a dataset from the Atmospheric Infrared Sounder (AIRS) on the Aqua satellite, Warner et al. (2016) evaluated a comprehensive monitoring of 13-year global tropospheric NH_3 distribution. Spatiotemporal patterns from satellite data suggested that the main source of atmospheric NH_3 was from farming and animal husbandry activities involving reactive N derived from synthetic N fertilizer use (Warner et al., 2017). Nevertheless, there are several limitations of previous studies that applied satellite data. First, most studies primarily relied on a national-level, one-year synthetic N fertilizer application map and ignored information on livestock manure management across the US. Second, how changes in spatiotemporal patterns of synthetic N fertilizer application and livestock manure management affect atmospheric NH_3 concentration across the US is still an open question. Third, most previous studies used a global linear regression model to explore relationships between NH_3 and driving factors, where the regression coefficient for each forcing factor remained constant across space and time (Chu et al., 2015; Hou et al., 2015). However, spatiotemporal non-stationarity exists in NH_3 and associated forcing variables. In addition, although hot and dry summers were found to be associated with high NH_3 concentrations in the Midwest (Warner et al., 2017), such relationships have not been examined in other US regions. Furthermore, Warner et al. (2017) may have overlooked potential underlying mechanisms that favored increases in atmospheric NH_3 across the US. Finally, climate change (e.g., increasing temperature) could exacerbate NH_3 emissions from highly fertilized croplands (Xu et al., 2019; Shen et al., 2020a, 2020b; Ma et al., 2021). Possible interactions between N additions and climate change have been largely ignored in previous work (Warner et al., 2017).

To address these limitations, the current study applied a satellite-based, 14-year monthly NH_3 dataset to explore change in spatiotemporal NH_3 patterns and the empirical relationships with synthetic N fertilizer application, livestock manure production, and climate factors across the US at both regional and pixel levels (Fig. 1). To reveal spatiotemporal variations of these relationships, this study used a GTWR model in an attempt to answer the following questions: 1) What was the spatiotemporal change pattern of NH_3 from 2002 to 2016? 2) What were the empirical associations of NH_3 with anthropogenic and climatic variables? 3) How did empirical associations evolve across space and time? and 4) What were potential physical mechanisms underlying changing NH_3 patterns?

The rest of the paper is organized as follows: In Section 2, we describe the data used in this study, including satellite-based NH_3 measurements, climate (i.e., temperature and precipitation), synthetic N fertilizer, and livestock manure. We also explain the statistical methods of trend analysis, correlation analysis, and GTWR. Section 3 presents the results of spatiotemporal associations between NH_3 concentration and three impact factors; limitations and future directions of study are also discussed. Section 4 is the conclusion.

2. Materials and methods

2.1. Data

Five spatially and temporally explicit datasets for the entire US were used: 1) monthly satellite-based NH_3 measurements, 2) monthly

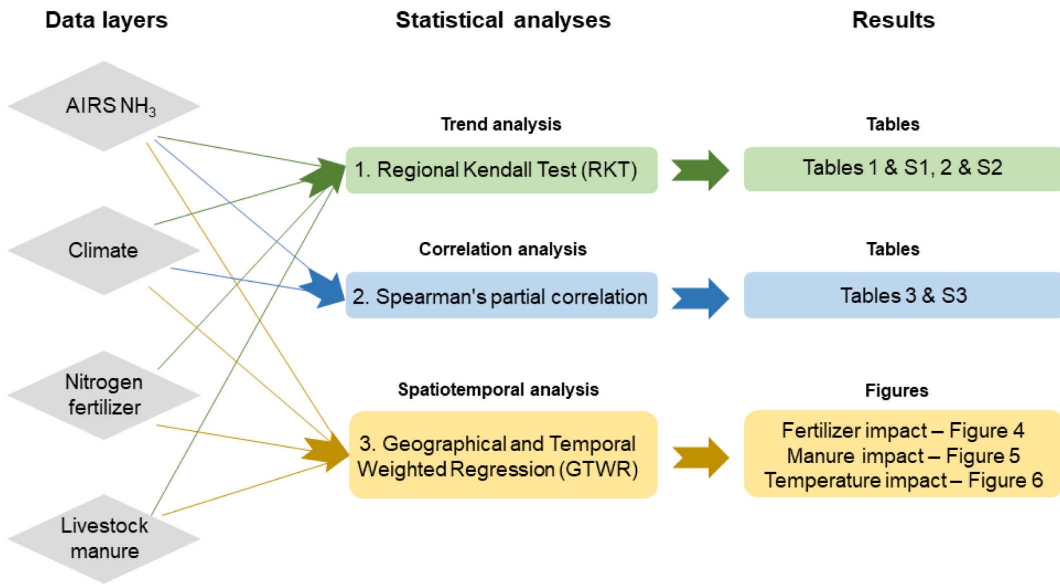

Fig. 1. Flowchart of the methodology for investigating spatiotemporal changes in NH_3 concentrations.

temperature, 3) monthly precipitation, 4) annual synthetic N fertilizer application, and 5) annual livestock manure production. Atmospheric NH_3 concentrations (September 2002 to August 2016) were obtained from AIRS. Validating against *in situ* data, vertical profiles of AIRS NH_3 were found to have small biases (within ~5–15% of retrieved profiles) in central California, despite possible biases associated with spatial resolution differences between the two instruments (Warner et al., 2016). The AIRS NH_3 products provide NH_3 volume mixing ratios (VMRs) at multiple levels from 500 hPa to the surface at a spatial resolution of 1° × 1°. More detailed information regarding the AIRS NH_3 retrieval method can be found in Warner et al. (2016, 2017). In this study, we selected NH_3 VMRs at 918 hPa (i.e., peak sensitivity) according to Warner et al. (2017). Surface temperature and precipitation from 2002 to 2016 were obtained from Daily Surface Weather Data version 3 (Daymet; Thornton et al. (2016)) with a spatial resolution of 1 km. Daymet generated daily weather and climatology variables through interpolating and extrapolating ground-based observations using statistical modeling techniques (Thornton et al., 2016). A spatially explicit data set of synthetic N fertilizer use during 2002–2015 was obtained from Cao et al. (2018) at a spatial resolution of 5 km × 5 km. Spatially explicit livestock manure production between 2002 and 2016 was obtained from Bian et al. (2021) at a spatial resolution of 30 s × 30 s. Climatic, N fertilizer, and manure datasets were aggregated into 1° × 1° grids to be consistent with NH_3 data.

2.2. Statistical analysis

We applied the non-parametric Regional Kendall Test (RKT) to examine overall trends of atmospheric NH_3 concentrations and four driving factors (i.e., temperature, precipitation, synthetic N fertilizer, and livestock manure production) for five regions and the entire US. The five regions were the West, Midwest, Mid-South, Southeast, and Northeast (Fig. 2a). To explore associations of NH_3 with mean monthly temperature (MMT) and precipitation (MMP), we performed a non-parametric Spearman's partial correlation. Trend and correlation analyses were carried out in R software for Windows (version 4.0.3, www.r-project.org/). The RKT was performed using the 'RKT package' with the estimated Theil-Sens slope (Marchetto et al., 2013). The Spearman's partial correlation was performed using the 'ppcor package' (Kim, 2015).

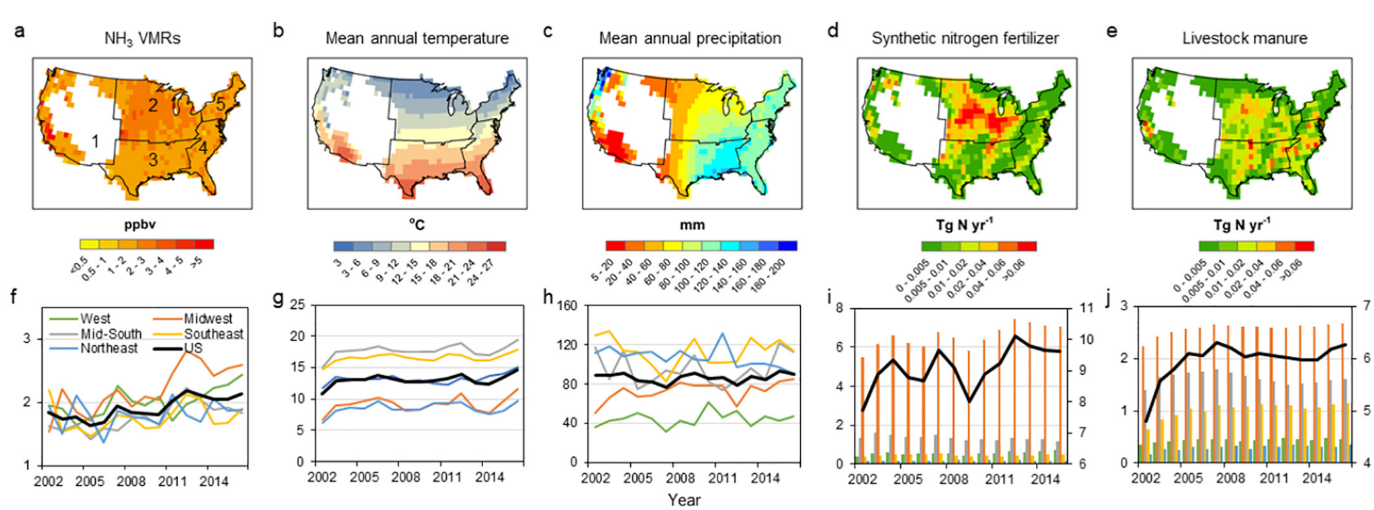

Fig. 2. Spatial distribution and temporal trends of NH_3 VMRs, mean annual temperature (MAT), mean annual precipitation (MAP), synthetic N fertilizer, and livestock manure production from 2002 to 2016. Top panels show the spatial pattern, while bottom panels show temporal changes. Panel numbers (i.e., 1, 2, 3, 4, and 5) in (a) represent the West, Midwest, Mid-South, Southeast, and Northeast regions of the US, respectively.

2.3. The GTWR model

To reveal magnitudes of N fertilizer, livestock manure, and climatic impacts on NH_3 and how such magnitudes change across space and time, this study applied GTWR at an annual scale for each grid cell in the US. As an extension of a traditional regression model, the GTWR model can simultaneously consider both spatial and temporal heteroscedasticity and thus provide spatiotemporal estimations (Chu et al., 2015; Huang et al., 2010; Wu et al., 2019). The GTWR model can be described as:

$$Y_i = \beta_0(u_i, v_i, t_i) + \sum_k \beta_k(u_i, v_i, t_i) X_{ik} + \varepsilon_i \quad (1)$$

where Y_i is the dependent variable of the ith sample (i.e., NH_3 in this study), X_{ik} are the independent variables of the ith sample (i.e., N fertilizer, livestock manure, climate variables in this study), u_i, v_i, and t_i are the space-time coordinates of the ith sample, and $\beta_k(u_i, v_i, t_i)$ is the estimated coefficient of the kth independent variable for the ith sample. The weighted least squares (WLS) approach was adopted to calibrate GTWR (Huang et al., 2010). The matrix expression for the estimated coefficient of the ith sample can be expressed as:

$$\widehat{\beta}_k(u_i, v_i, t_i) = \left[X^T W(u_i, v_i, t_i) X\right]^{-1} X^T W(u_i, v_i, t_i) Y \quad (2)$$

where $W(u_i, v_i, t_i)$ is a spatiotemporal weight matrix that can be measured using a variety of distance-decay functions, such Gaussian, bi-square, and exponential functions. In this study, we used a Gaussian kernel function (Huang et al., 2010):

$$W_{ij}^{ST} = \exp\left[\left(\frac{d_{ij}^{st}}{h^{st}}\right)^2\right] \quad (3)$$

where d_{ij}^{st} is the spatiotemporal distance between samples i and j, and $(d_{ij}^{st})^2 = \lambda[(u_i - u_j)^2 - (v_i - v_j)^2] + \mu(t_i - t_j)^2$. Here, λ and μ are scale factors used to balance difference effects employed to measure spatial and temporal distances in their respective metric systems, and h^{st} is the spatiotemporal bandwidth and $h^{st} = h^s + \varphi * h^t$. The optimal spatial bandwidth h^s and temporal bandwidth h^t can be obtained using a corrected version of the Akaike information criterion (AICc) (Hurvich et al., 1998).

To make direct comparisons among different covariates, we standardized dependent and independent variables using the 'scale' function in R. We also compared the R-square (R^2) from GTWR with that from the global regression model (i.e., ordinary least squares (OLS)) to assess GTWR performance. We selected NH_3 as the dependent variable and N fertilizer, livestock manure, and temperature as independent variables for both GTWR and OLS models. The selection was described in Section 3.3. The GTWR and OLS simulations were conducted using the GTWR AddIn in ESRI ArcMap 10.8 developed by Huang et al. (2010).

3. Results and discussion

3.1. Trends in NH_3 concentrations and driving factors for five US regions

Across the US, atmospheric NH_3 concentrations significantly increased by 0.030 ppbv yr^{-1} between 2002 and 2016 (Table 1). The US Midwest has been identified as a global hotspot for NH_3 emissions based on satellite observations (Griffis et al., 2019; Shephard et al., 2011; Van Damme et al., 2020). We found that the Midwest had the highest NH_3 concentrations among all five regions (Fig. 2f) with the largest rate increase of 0.074 ppbv yr^{-1} (p-value <0.01). This was consistent with previous studies (e.g., 0.056 ppbv yr^{-1}, Warner et al. (2017)). In addition, our analysis of ARIS NH_3 trends in the Midwest (3.8%, a compound annual growth rate) was in line with trends obtained from the IASI-NH_3 dataset during 2008–2018 (3.42% ± 0.59%, Van Damme et al. (2020)). In contrast, the Southeast and Northeast showed slight increases in annual NH_3 concentrations that were not statistically significant (p-value = 0.11 and 0.55, respectively). The Mid-South and West regions showed a medium increase in NH_3 concentrations with rates of 0.030 ppbv yr^{-1} (p-value <0.01) and 0.038 ppbv yr^{-1} (p-value <0.01), respectively (Table 1). At monthly scales, NH_3 concentration trends were broadly consistent with those of annual scales (Table 1); however, the significance of NH_3 concentrations in the Southeast and Northeast regions increased (Table 1). This was likely associated with the growing frequency of extreme high NH_3 concentrations in later years due to climate variability. For example, we found that the highest value of 5.2 ppbv in April 2011 in the Northeast was smoothed out in the annual mean value (Figs. 2f & 3e), thus there was no observable increase in annual NH_3 concentrations.

Table 1
Regional Kendall test of regional trends for atmospheric NH_3 concentrations in the US from 2002 to 2016.

Region	Monthly		Annual	
	Slope	p	Slope	p
West	0.032	<0.001	0.038	<0.01
Midwest	0.043	<0.001	0.074	<0.01
Mid-South	0.033	<0.001	0.030	<0.01
Southeast	0.013	<0.050	0.015	0.11
Northeast	0.026	<0.050	0.010	0.55
The United States	0.028	<0.001	0.030	<0.05

Mean annual temperatures (MAT) during the study period were much higher across southern regions (i.e., Mid-South and Southeast) compared to northern regions (i.e., Midwest and Northeast) (Fig. 2b), which was expected due to latitudinal effects of solar radiation. In terms of mean annual precipitation (MAP), the Northeast and Southeast were higher than remaining regions, especially the western US (Fig. 2c). Rainfall patterns were mainly due to topography of the West and moisture from the Gulf of Mexico for the East (Hu et al., 1998; Karl and Knight, 1998). Overall, there were no statistically significant trends in mean annual and monthly temperature and precipitation across the five regions from 2002 to 2016 (Tables S1, S2). However, both temperature and precipitation exhibited large intra- and inter-annual variability for this period (Figs. 2g, h & 3).

Hotspots of synthetic N fertilizer use were concentrated in the Midwestern US, the Mississippi Valley, and some regions of the Western US (e.g., California) (Fig. 2d). In contrast, hotspots of livestock manure production were spread across all five regions with a much higher amount detected in the states of California, North Carolina, Iowa, and Arkansas (Fig. 2e). The total amount of US fertilizer use increased at a rate of 0.092 Tg N yr^{-1} (p-value <0.05) from 2002 to 2015 (Table 2), however, with annual fluctuations (Fig. 2i). For example, the substantial drop in fertilizer consumption between 2008 and 2009 was largely associated with the high price of fertilizer caused by the 2008 financial crisis (USDA-ERS, 2013). The Midwest, accounting for ~80% of the total national fertilizer consumption, dominated the increase across the US during the study period (Fig. 2i). The national total manure production depicted a rapid increase from 2002 to 2008 and then roughly remained constant thereafter (Fig. 2j). At the regional scale, with the exception of the Mid-South, the remaining four regions showed statistically significant increases in livestock manure production for the period of 2002–2016 (Table 2). The Midwest was the largest contributor to national total manure production, followed by the Mid-South and Southeast (Fig. 2j).

3.2. Monthly NH_3 concentration response to climate factors

Spearman's partial correlation analyses revealed that monthly atmospheric NH_3 concentrations were positively correlated with monthly surface temperature in the five US regions (Table 3). The highest correlation coefficient was noted in the Mid-South (r-value = 0.651), followed by the Midwest (r-value = 0.272) and West (r-value = 0.262) regions. In contrast, only the Mid-South showed a significantly

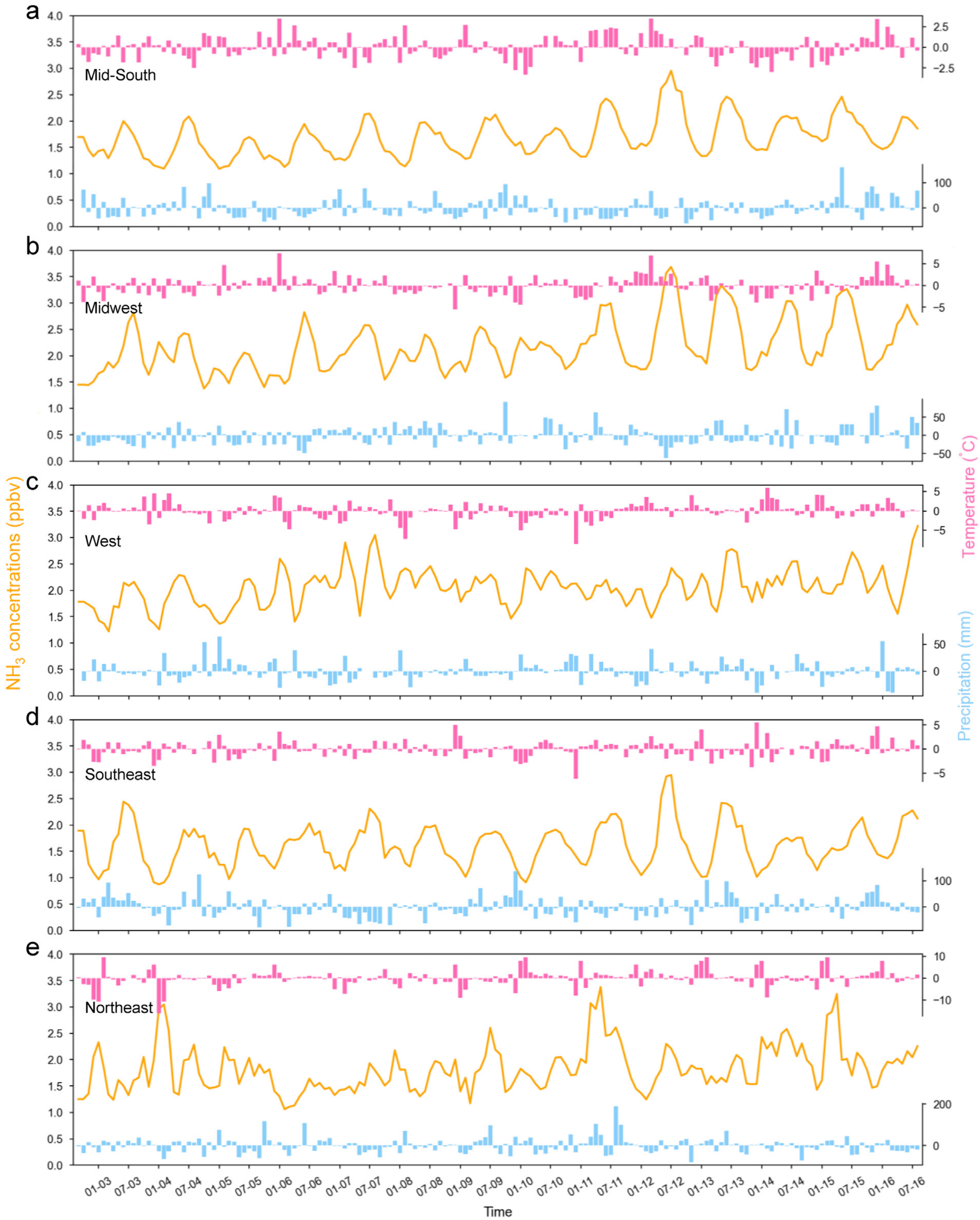

Fig. 3. Temporal changes in monthly NH_3 concentrations, temperature anomalies, and precipitation anomalies in the five US regions from 2002 to 2016. Monthly NH_3 concentrations are shown as 5-month moving averages. Monthly temperature and precipitation anomalies were calculated by subtracting the 14-year average of each month.

positive correlation between precipitation and atmospheric NH_3 concentrations (Table 3).

Consistent with high-resolution maps of IASI NH_3 seasonality and AMoN (Wang et al., 2021), a single summer peak was observed from AIRS NH_3 in the Mid-South. There were higher peak temperatures in summers of 2011 and 2012 in the Mid-South, and elevated NH_3 concentrations were also detected during this period (Fig. 3a). We also saw a peak NH_3 concentration in the summer of 2015 that coincided with extremely heavy rainfall (Fig. 3a). This could be due to rice production since rice is the third largest among cereals (after corn and wheat) in the US and 80% of rice farms are located in the Mid-South (USDA, NASS). Ma et al. (2021) pointed out that rice cultivation served as the leading background source of NH_3 emissions due to high temperatures and waterlogging. In our study, we found a significantly positive correlation between MMP and atmospheric NH_3 concentrations in the Mid-South (Table 3, p-value <0.01). Rice cultivation requires a substantial

Table 2
Regional Kendall test of regional trends for synthetic N fertilizer and livestock manure production in the US from 2002 to 2016.

Region	Fertilizer		Manure	
	Slope	p	Slope	p
West	0.015	<0.05	0.005	<0.05
Midwest	0.092	<0.05	0.014	<0.05
Mid-South	−0.022	<0.05	−0.011	0.276
Southeast	0.002	<0.05	0.006	<0.05
Northeast	0.004	0.346	0.018	<0.001
The United States	0.092	<0.05	0.026	0.198

amount of water either from irrigation or from rainfall, and sufficient water supply favors NH_3 releases since urea can react with water and the urease enzyme to produce ammonium carbonate (unstable compound that quickly decomposes to release NH_3 gas).

The positive correlation between surface temperature and NH_3 found in the Midwest was in conformity with Warner et al. (2017) who reported that high average surface temperatures in the US Midwest could facilitate NH_3 emissions. The positive feedback between NH_3 concentrations and temperature was also supported by Hu et al. (2021), who found that NH_3 emissions peaked from May to July in 2017 in the US Corn Belt by combining tall tower, ground-based measurements, and modeling. In addition, a 2.5 °C–3.6 °C higher air temperature led to abnormally higher NH_3 concentrations in May 2018 compared to other months in the study region. We observed that high NH_3 concentrations in 2012 coincided with high summer temperature and low rainfall (Fig. 3b), which was supported by Warner et al. (2017) where hot and dry summers were conducive to high NH_3 concentrations. However, this pattern did not persist across years. For example, our results for 2011 showed a similarly high NH_3 concentration in summer with heavy rainfall (Fig. 3b). Table 3 shows a weak relationship between NH_3 concentrations and MMP in the Midwest, which may indicate that other factors such as soil moisture, pH, and soil inorganic N content could also affect monthly variations in NH_3 concentration.

The West region received minimal annual rainfall and was the driest area in the US (Figs. 2c, h). We found a significantly positive correlation between surface temperature and NH_3 in this region (Table 3). Time-series temperature data revealed that winters in the West became warmer since 2011 despite summer temperatures being similar during 2002–2016 (Fig. 3c). Increased NH_3 released from livestock manure during warmer winters possibly contributed to increased annual NH_3 concentrations.

In the Northeast and Southeast, positive correlations between surface temperature and NH_3 were weak. For the Northeast, many missing monthly NH_3 concentration values may have affected correlation analysis results. For the Southeast, there were peak NH_3 concentrations in summers due to high temperatures (Fig. 3d). Annual rainfall in the Northeast and Southeast were much higher than in remaining US regions, and heavy rainfall usually occurred in summer months. Frequent rainfall events could have washed livestock manure into riverine ecosystems, leading to low NH_3 emissions in both regions.

Table 3
Summary of Spearman's partial correlation test for monthly mean temperature and precipitation with NH_3 concentration.

Region	Correlation coefficient	
	NH_3 ~ MMT	NH_3 ~ MMP
West	0.262***	0.039
Midwest	0.270***	0.109
Mid-South	0.651***	0.213**
Southeast	0.210***	0.001
Northeast	0.201**	0.017
The United States	0.510***	0.156**

** Indicates statistical significance at 0.01 level.
*** Indicates statistical significance at 0.001 level.

It is worth noting that large discrepancies remain in monthly NH_3 concentrations observed from different satellites. High-resolution NH_3 column maps from IASI found that springs exhibited the maximum level of NH_3 concentrations, which was consistent with fertilizer application timing in the Midwest (Wang et al., 2021), while summer peaks detected by AIRS in our study were consistent with measurements from AMoN. Unlike the narrow summer peaks of IASI NH_3 in the western US (Wang et al., 2021), AIRS NH_3 showed bimodal peaks (one in both summer and winter) or relatively insignificant seasonal variability in some years (Fig. 3c). This large discrepancy is partially attributed to missing data and much coarser spatial resolution of the AIRS NH_3 product. Similar to the western US, AIRS NH_3 did not show obvious single peaks in the Northeast and Southeast for most years (Fig. 3e). However, AIRS NH_3 cannot be directly compared with IASI and AMoN due to large inconsistencies in geographic coverage of areas in both regions (Wang et al., 2021).

3.3. Impacts of anthropogenic and climatic variables on NH_3 concentrations

We ran the GTWR model at the annual scale to examine magnitudes of anthropogenic and climatic influences on annual NH_3 concentrations and how such magnitudes change spatiotemporally from 2002 to 2015. In addition, precipitation was excluded in the GTWR model since there were no significant correlations of NH_3 concentrations with precipitation across most regions of the US (Section 3.2, Table 3). The following analyses only focused on three driving factors (i.e., N fertilizer, livestock manure, and temperature).

Figs. 4–6 present the spatiotemporal coefficients computed by the GTWR model for individual driving factors for each grid cell across the US. Our results indicated that the GTWR model reasonably captured the effects of the three driving factors on annual NH_3 concentrations; the overall R^2 (~0.205) was much higher compared to the OLS regression (R^2 = ~0.061). From a regional perspective, the Midwest experienced the most intensive agricultural activities since it received ~80% of total N fertilizer and accounted for about half of total US manure production (Fig. 2i, j) (Bian et al., 2021; Cao et al., 2018). Thus, a substantial amount of reactive N was available for release as NH_3 gas in this region. We found that livestock manure had a consistent positive impact on NH_3 concentrations spatiotemporally with coefficients ranging from 0 to 0.4 (Fig. 4). However, this effect slightly decreased along with declining stable manure production after 2008 (Fig. 2j). A consistent higher effect of manure was detected in the western part of the Midwest (i.e., Kansas), which had higher temperatures and less precipitation. Nitrogen fertilizer application was another reason for higher NH_3 concentrations in the Midwest and its effects continued to enlarge during 2002–2015 with coefficients ranging from −0.2 to 0.6 (Fig. 5). We observed a continuous rise in the effect of N fertilizer in northern parts of the Midwest (i.e., Northern Great Plains) that was largely associated with increased fertilizer consumption for spring wheat and corn production (Cao et al., 2020).

Our results also revealed that the influence of temperature on temporal evolution of NH_3 concentrations was associated with synthetic N fertilizer use in the Northern Great Plains. Temperature had a positive effect on NH_3 concentrations with coefficients as high as 0.8 in the northwestern Midwest, while this effect was weak and ranged from −0.4 to 0 in the eastern Midwest (Fig. 6). This contrasting effect of temperature was highly associated with opposing fertilizer usage (decrease in the eastern Midwest and a rapid increase in the northwest). Our study notably provided evidence that synthetic N fertilizer interaction with temperature could stimulate NH_3 release (especially in more vulnerable regions like the Northern Great Plains), which was neglected in previous studies (Cao et al., 2018; Li et al., 2017; Nair et al., 2019; Warner et al., 2017; Yu et al., 2018). A recent study also observed an increase over some source regions in the US Midwest in summers due to increased temperatures and certain farm practices that promoted greater NH_3 volatilization (Shephard et al., 2020). Additionally, the Coupled Model Intercomparison Project Phase 6 (CMIP6) ensemble

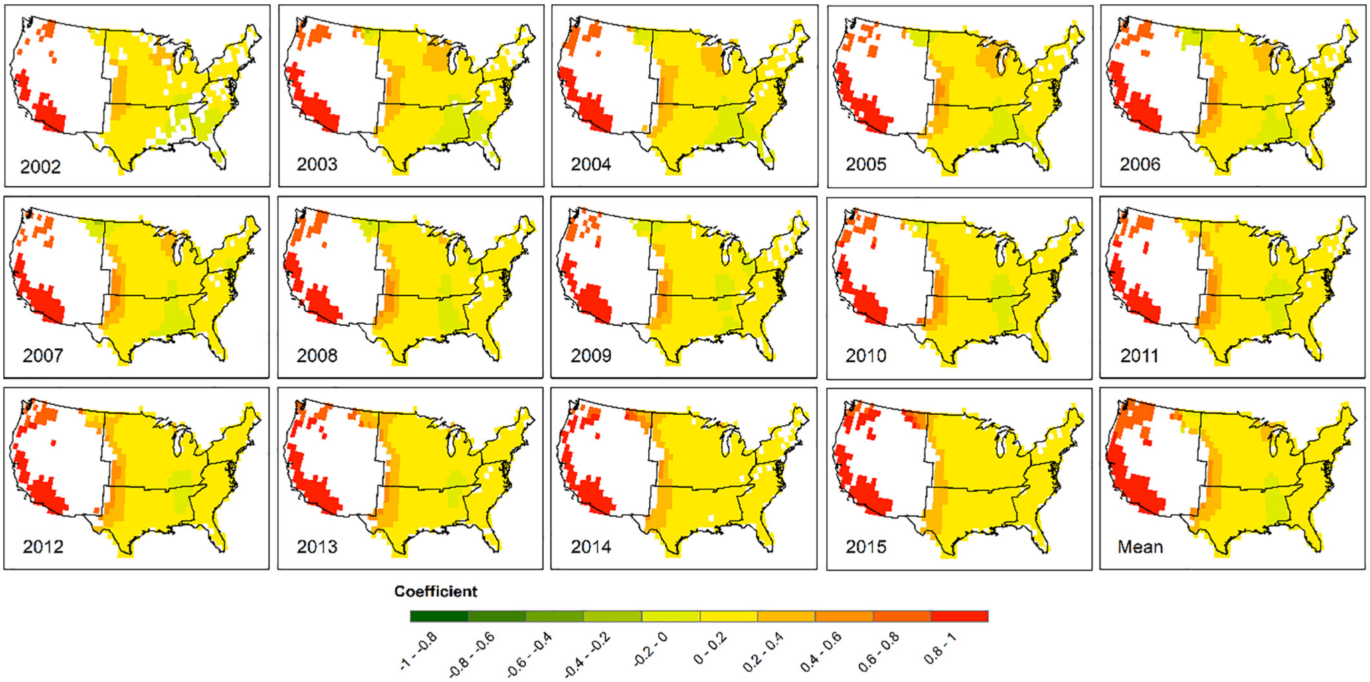

Fig. 4. Spatiotemporal impacts of livestock manure on NH_3 concentration for each grid cell during 2002–2015. The last panel is the mean of climatological coefficients.

showed a significant increase in MAT across the US with more pronounced rises in the northern half during 2021–2099 under all three Shared Socioeconomic Pathways (SSPs) (Almazroui et al., 2021). Thus, global warming interactions with substantial N additions could lead to higher NH_3 concentrations and decreased air quality in the US Midwest for the remainder of the century. This is confirmed by a recent study by Shen et al. (2020a) who predicted substantial increases in future NH_3 emissions for the Corn Belt and Northern Great Plains (i.e., Midwest in our study) by 2100 in the RCP8.5 climate scenario (i.e., the highest projected emission scenario). Moreover, Hu et al. (2020) found that peak NH_3 emissions from the US Corn Belt in November 2017 were associated with above-normal air temperature. Their results imply that future warmer fall temperatures could stimulate agricultural NH_3 emissions in the midwestern US due to dense livestock operations and high synthetic nitrogen fertilizer usage.

Followed by the Midwest, the Mid-South also experienced intensive agricultural activities that introduced a considerable amount of reactive N available for loss in the form of NH_3 (Fig. 2i, j). Livestock manure showed persistent positive impacts on NH_3 concentrations across time and space in the Mid-South (coefficients ranging from 0 to 0.2), except for some eastern parts of this region (Fig. 4). Patterns and magnitudes were similar to the Midwest. In addition, there was a spatiotemporal-consistent pattern of positive effects of N fertilizer on NH_3 concentrations in the Mid-South with coefficients ranging from 0 to 0.6 (Fig. 5). The

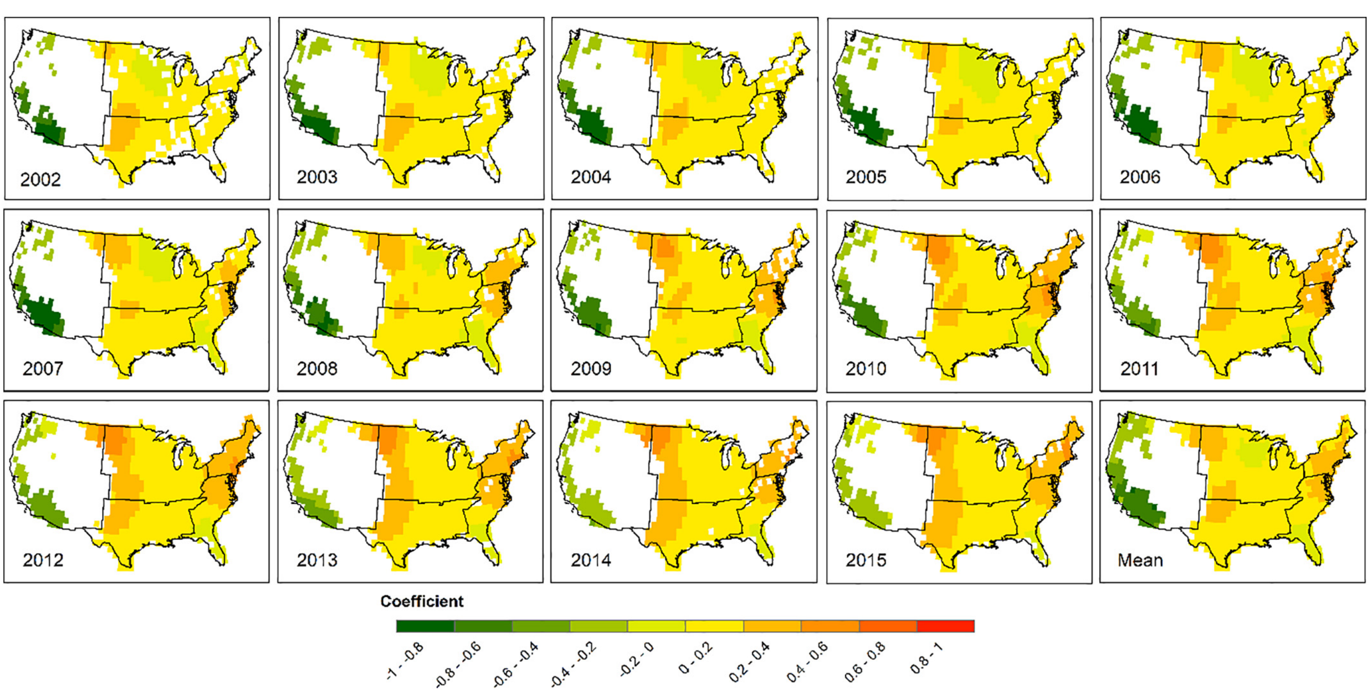

Fig. 5. Spatiotemporal impacts of synthetic N fertilizer on NH_3 concentration for each grid cell during 2002–2015. The last panel is the mean of climatological coefficients.

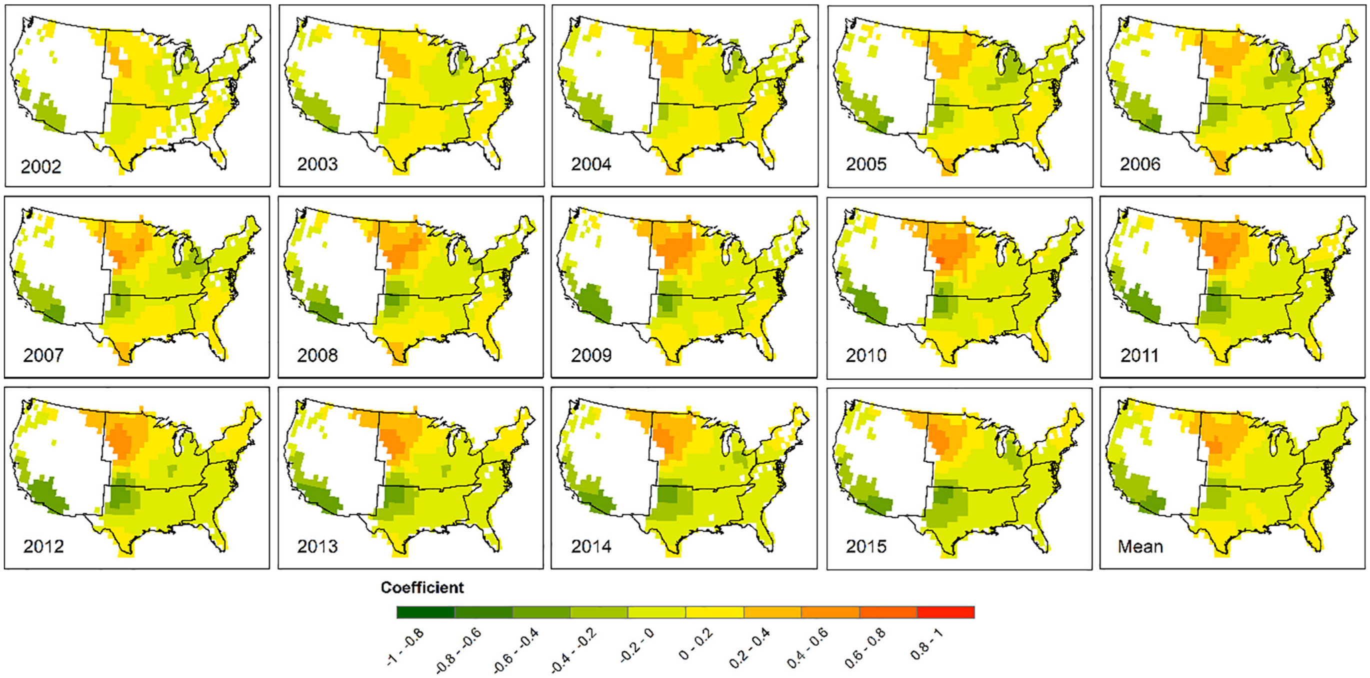

Fig. 6. Spatiotemporal impacts of annual mean temperature on NH_3 concentration for each grid cell during 2002–2015. The last panel is the mean of climatological coefficients.

impacts of temperature on NH_3 concentrations were positive across central and southern parts of the Mid-South with coefficients ranging from 0 to 0.2 before 2010. High temperature could be a trigger for increased NH_3 emissions from rice and other crop cultivations receiving intensive N fertilizer and manure applications in these two parts of the Mid-South. Shen et al. (2020a) predicted that the Southern Plains and Delta States (i.e., the Mid-South in this study) would experience a considerable increase in NH_3 emissions by 2100 in the RCP8.5 scenario when N input was fixed at the 2010 level. Consistent with Shen et al. (2020a), our study indicated that this region would possibly become high NH_3 concentration hotspots in the context of climate warming. However, this effect gradually diminished in these two parts of the Mid-South (Fig. 6), indicating that contribution of other factors (e.g., manure) increased (Fig. 4). In contrast, there was a persistent weak impact of temperature on NH_3 with coefficients ranging from −0.6 to 0 (Fig. 6) in northwestern parts of the Mid-South, while manure and N fertilizer contributions were relatively higher (Figs. 4–5), indicating that manure and N fertilizer were the main driving factors for the NH_3 variability in the northwestern portions of this region.

Most of the West region lacked data due to high elevation (above the 918 hPa level that data are not shown) or weeks of persistent cloud coverage (Warner et al., 2016), thus leaving only coefficients for northeastern Montana and western coastal areas that include California, Oregon, and Washington (Figs. 4–6). Livestock manure had consistent positive impacts on NH_3 concentrations spatiotemporally in the western coastal region, with coefficients larger than 0.8 (Fig. 4). High manure influence in this area was largely attributable to considerable NH_3 emissions from livestock farming. Furthermore, hot and dry weather conditions might trigger more NH_3 gas release from manure. Consistent with our findings, Van Damme et al. (2018) identified several agricultural NH_3 emission hotspots in California based on a high resolution map monitored by IASI satellite. Hotspots due to pig farms in Utah were also detected by Van Damme et al. (2018), but were not shown in our study due to missing data. In addition, Li et al. (2017) observed the highest NH_3 concentrations near large concentrated animal feeding operations (CAFO) in Colorado when using Radiello passive NH_3 samplers. However, this was not captured by NASA AIRS NH_3 products (Warner et al., 2017) due to missing data in our study. Winters in the West were getting warmer since 2011 despite summer temperatures remaining similar during 2002–2016 (Fig. 3c). Thus, more NH_3 releases from livestock manure during warmer winters possibly contribute to increased annual NH_3 concentrations (Amon et al., 2001; Misselbrook et al., 2016; Sutton et al., 2013). The influence of N fertilizer and temperature on NH_3 concentrations had a persistent weak pattern in the western coastal regions; however, both coefficients increased from 2002 to 2015 (Figs. 5–6). This was associated with a continuous increase in fertilizer consumption (Cao et al., 2018) along with temperature (Thornton et al., 2016) in both regions. Similar to our findings for the Northern Great Plains, warming interactions with increased fertilizer consumption led to a continuous increase in NH_3 emissions from this region.

Similar to the aforementioned three regions, impacts of livestock manure on NH_3 concentrations were positive spatiotemporally in the Southeast and Northeast, with coefficients ranging from 0 to 0.2 (Fig. 4). Although there were numerous hotspots of high livestock manure production in the eastern part of the US from CAFO (Bian et al., 2021), both regions had much smaller manure influences compared to the West. In contrast to California which was dry and hot, the eastern US was hot and humid due to year-round rainfall events. Heavy rainfall can wash livestock manure into nearby riverine systems resulting in less NH_3 available for release as NH_3 gas (Sinha and Michalak, 2016). For example, there was a measurable effect of CAFO waste manures (typically swine) on water quality in many North Carolina Coastal Plain streams (Harden, 2015). We observed an overall positive pattern of N fertilizer (coefficients ranging from 0 to 0.6) but a weak temperature impact (coefficients ranging from −0.2 to 0) in the Northeast and Southeast (except for Florida) during 2002–2015 (Figs. 4–5). Before 2008, the effect of temperature was positive in most regions of the Southeast (coefficients ranging from 0 to 0.2), and this effect decreased (coefficients ranging from −0.2 to 0) thereafter (Fig. 6).

3.4. Limitations

In this study, we examined the impacts of four driving factors on spatiotemporal changes in NH_3 concentrations across the US. However, there were several limitations relevant to the driving data and the GTWR model that should be noted. First, the data quality of AIRS NH_3 products with a spatial resolution of $1° \times 1°$ might be too coarse to identify hotspots of NH_3 concentrations associated with local farm operations. Van Damme et al. (2018) successfully identified 248 hotspots with diameters smaller than 50 km globally, which served as a significant reference for policy makers to effectively manage NH_3 emissions at farm- or local-scales. In addition, there were many missing pixels in the western US that experienced high agricultural activities and had hotspots identified in other studies (Li et al., 2017; Van Damme et al., 2018). The missing data were either due to high elevation (above the 918 hPa level that data are not shown) or persistent cloudy days (Warner et al., 2016). While there were many missing data for the Western US, the AIRS product still successfully provided estimates for key NH_3 emission hotspots (i.e., California, Montana, and Washington). Although this was consistent with Van Damme et al. (2018), who used a high-resolution map obtained from IASI satellite observations, they also identified Colorado and Utah as hotspots. Second, Spearman's partial correlation analyses revealed that monthly atmospheric NH_3 concentrations were positively correlated with monthly surface temperature in the five US regions (Table 3). However, these strong correlations were not detected between MAT and NH_3 concentrations (Table S3). Using annual datasets of temperature might decrease the confidence of GTWR analysis. Once available, future work should take monthly fertilizer and manure datasets into consideration. Last, due to non-stationarity of the model, GTWR might simulate unexpected abrupt changes in coefficients (Huang et al., 2010). For example, the contrasting temperature coefficient signs in 2009 and 2010 for the Southeast indicates a need for further evaluations.

In addition, there are other factors that could be important for explaining changes in NH_3 concentrations. The R^2 from GTWR was ~0.205, indicating that three driving factors only explain ~20.5% of the variability in the dependent variable (i.e., NH_3 concentrations). The decline in atmospheric SO_2 and NO_x emissions due to U.S. regulations partially contributed to increased NH_3 concentrations across the US in recent decades (Van Damme et al., 2020; Warner et al., 2017; Yu et al., 2018). Thus, spatiotemporal changes in SO_2 and NO_x emissions should be included in the GTWR model in our future efforts. Although agricultural activities accounted for over 80% of NH_3 emissions (Bouwman et al., 2002), the bi-directional NH_3 exchange module indicates that crop canopy tends to absorb some of the released NH_3 from fertilized soils (Bash et al., 2013; Nemitz et al., 2001). Thus, crop types and phenology stages could be important factors regulating NH_3 releases from synthetic N fertilizer and manure applications (Xu et al., 2019). In addition, agricultural management strategies (e.g., tillage, irrigation) could affect soil properties (e.g., pH, soil moisture) that further impact NH_3 emission patterns (Ma et al., 2021; Xu et al., 2019; Zhan et al., 2021). Failure to account for the above-mentioned factors could introduce large uncertainties when attempting to explain spatiotemporal changes in NH_3 concentrations.

4. Conclusions

This study is one of the first attempts to investigate the causes of spatial and temporal changes in satellite-derived atmospheric NH_3 concentrations based on a GTWR model driven by spatially-explicit datasets of synthetic N fertilizer application, livestock manure production, and climate factors. Across the US, atmospheric NH_3 concentrations have significantly increased by 0.030 ppbv yr^{-1} between 2002 and 2016. The highest increase was observed in the Midwest, followed by the Mid-South and West regions.

Reasons for these spatiotemporal changes in NH_3 concentrations were diverse. Livestock manure and N fertilizer had consistent positive impacts on NH_3 concentrations spatiotemporally in most regions of the Midwest. We observed a continuous rise in the effect of N fertilizer in northern portions of the Midwest (i.e., Northern Great Plains) largely due to increased fertilizer consumption for spring wheat and corn production. In addition, our results showed that the interactive effect between synthetic N fertilizer and temperature might stimulate the release of NH_3, especially in more vulnerable regions like the Northern Great Plains. In most areas of the Mid-South, high temperature could be a trigger for increased NH_3 emissions from rice and other crop cultivations receiving intensive N fertilizer and manure applications. The high influence of manure in the West was largely attributable to considerable NH_3 emissions from livestock farm operations in this region. In addition, hot and dry weather might trigger more NH_3 gas release from manure. The Southeast and Northeast depicted much smaller spatiotemporally positive influences of manure compared to the West, presumably due to frequent rainfalls in both regions washing livestock manure into nearby riverine systems resulting in less NH_3 available for release.

Nomenclature

NH_3	ammonia
N	nitrogen
NO_x	nitrogen oxides
AMoN	Atmospheric Deposition Program Ammonia Monitoring
IASI	Infrared Atmospheric Sounding Interferometer
NADP	National Atmospheric Deposition Program
GTWR	geographical and temporal weighted regression
AIRS	Atmospheric Infrared Sounder
VMRs	volume mixing ratios
RKT	Regional Kendall Test
MMT	mean monthly temperature
MMP	mean monthly precipitation
WLS	weighted least squares
AICc	corrected version of the Akaike information criterion
R^2	R-square
OLS	ordinary least squares
MAT	mean annual temperatures
MAP	mean annual precipitation
CMIP6	Coupled Model Intercomparison Project Phase 6
SSPs	Shared Socioeconomic Pathways
CAFO	concentrated animal feeding operations

CRediT authorship contribution statement

Yaqian He: Methodology, Software, Formal analysis, Investigation, Writing – original draft, Writing – review & editing. **Rongting Xu:** Conceptualization, Methodology, Software, Formal analysis, Investigation, Writing – original draft, Writing – review & editing. **Stephen A. Prior:** Writing – review & editing. **Di Yang:** Visualization, Writing – review & editing. **Anni Yang:** Visualization, Writing – review & editing. **Jian Chen:** Data curation, Software.

Declaration of competing interest

The authors declare that they have no known competing financial interests or personal relationships that could have appeared to influence the work reported in this paper.

Acknowledgement

Y.Q.H. was partially supported by University of Central Arkansas University Research Council grant. R.T.X, Y.Q.H., D.Y., and J.C. were supported by a Microsoft AI for Earth Microsoft Azure Compute Grant.

Appendix A. Supplementary data

Supplementary data to this article can be found online at https://doi.org/10.1016/j.scitotenv.2021.147899.

References

Almazroui, M., Islam, M.N., Saeed, F., Saeed, S., Ismail, M., Ehsan, M.A., Diallo, I., O'Brien, E., Ashfaq, M., Martínez-Castro, D., Cavazos, T., Cerezo-Mota, R., Tippett, M.K., Gutowski, W.J., Alfaro, E.J., Hidalgo, H.G., Vichot-Llano, A., Campbell, J.D., Kamil, S., Rashid, I.U., Sylla, M.B., Stephenson, T., Taylor, M., Barlow, M., 2021. Projected changes in temperature and precipitation over the United States, Central America, and the Caribbean in CMIP6 GCMs. Earth Syst. Environ. 5, 1–24. https://doi.org/10.1007/s41748-021-00199-5.

Amon, B., Amon, T., Boxberger, J., Alt, C., 2001. Emissions of NH_3, N_2O and CH_4 from dairy cows housed in a farmyard manure tying stall (housing, manure storage, manure spreading). Nutr. Cycl. Agroecosyst. 60, 103–113. https://doi.org/10.1023/A:1012649028772.

Bash, J., Cooter, E., Dennis, R., Walker, J., Pleim, J., 2013. Evaluation of a regional air-quality model with bidirectional NH_3 exchange coupled to an agroecosystem model. Biogeosciences 10, 1635–1645. https://doi.org/10.5194/bg-10-1635-2013.

Bauer, S.E., Tsigaridis, K., Miller, R., 2016. Significant atmospheric aerosol pollution caused by world food cultivation. Geophys. Res. Lett. 43, 5394–5400. https://doi.org/10.1002/2016GL068354.

Bian, Z., Tian, H., Yang, Q., Xu, R., Pan, S., Zhang, B., 2021. Production and application of manure nitrogen and phosphorus in the United States since 1860. Earth Syst. Sci. Data 13, 515–527. https://doi.org/10.5194/essd-13-515-2021.

Bouwman, A., Boumans, L., Batjes, N., 2002. Estimation of global NH_3 volatilization loss from synthetic fertilizers and animal manure applied to arable lands and grasslands. Global Biogeochem. Cy. 16, 1024. https://doi.org/10.1029/2000GB001389.

Cao, P., Lu, C., Yu, Z., 2018. Historical nitrogen fertilizer use in agricultural ecosystems of the contiguous United States during 1850–2015: application rate, timing, and fertilizer types. Earth Syst. Sci. Data 10, 969–984. https://doi.org/10.5194/essd-10-969-2018.

Cao, P., Lu, C., Zhang, J., Khadilkar, A., 2020. Northwestward cropland expansion and growing urea-based fertilizer use enhanced NH_3 emission loss in the contiguous United States. Atmos. Chem. Phys. 20, 11907–11922. https://doi.org/10.5194/acp-20-11907-2020.

Chu, H.-J., Huang, B., Lin, C.-Y., 2015. Modeling the spatio-temporal heterogeneity in the PM10-PM2.5 relationship. Atmos. Environ. 102, 176–182. https://doi.org/10.1016/j.atmosenv.2014.11.062.

Clark, C.M., Tilman, D., 2008. Loss of plant species after chronic low-level nitrogen deposition to prairie grasslands. Nature 451, 712–715. https://doi.org/10.1038/nature06503.

Cullen, D.W., Guida, V., 2021. Use of geographically weighted regression to investigate spatial non-stationary environmental effects on the distributions of black sea bass (*Centropristis striata*) and scup (*Stenotomus chrysops*) in the Mid-Atlantic Bight, USA. Fish. Res. 234, 105795. https://doi.org/10.1016/j.fishres.2020.105795.

Davidson, E.A., David, M.B., Galloway, J.N., Goodale, C.L., Haeuber, R., Harrison, J.A., Howarth, R.W., Jaynes, D.B., Lowrance, R.R., Thomas, N.B., Peel, J.L., Pinder, R.W., Porter, E., Snyder, C.S., Townsend, A.R., Ward, M.H., 2011. Excess nitrogen in the US environment: trends, risks, and solutions. Iss. Ecol. 15, 1–16. http://www.esa.org/esa/wp-content/uploads/2013/03/issuesinecology15.pdf.

Du, E., 2016. Rise and fall of nitrogen deposition in the United States. Proc. Natl. Acad. Sci. U. S. A. 113, E3594–E3595. https://doi.org/10.1073/pnas.1607543113.

Du, E., de Vries, W., Galloway, J.N., Hu, X., Fang, J., 2014. Changes in wet nitrogen deposition in the United States between 1985 and 2012. Environ. Res. Lett. 9, 095004. https://doi.org/10.1088/1748-9326/9/9/095004.

Fotheringham, A.S., Crespo, R., Yao, J., 2015. Geographical and temporal weighted regression (GTWR). Geogr. Anal. 47, 431–452. https://doi.org/10.1111/gean.12071.

Fowler, D., Steadman, C.E., Stevenson, D., Coyle, M., Rees, R.M., Skiba, U., Sutton, M., Cape, J., Dore, A., Vieno, M., 2015. Effects of global change during the 21st century on the nitrogen cycle. Atmos. Chem. Phys. 15, 13849–13893. https://doi.org/10.5194/acp-15-13849-2015.

Griffis, T.J., Hu, C., Baker, J.M., Wood, J.D., Millet, D.B., Erickson, M., Yu, Z., Deventer, M.J., Winker, C., Chen, Z., 2019. Tall tower ammonia observations and emission estimates in the US Midwest. J. Geophys. Res.-Biogeo. 124, 3432–3447. https://doi.org/10.1029/2019JG005172.

Harden, S.L., 2015. Surface-Water Quality in Agricultural Watersheds of the North Carolina Coastal Plain Associated with Concentrated Animal Feeding Operations. Scientific Investigations Report, Reston, VA, p. 70. http://pubs.er.usgs.gov/publication/sir20155080.

Hong, Z., Mei, C., Wang, H., Du, W., 2021. Spatiotemporal effects of climate factors on childhood hand, foot, and mouth disease: a case study using mixed geographically and temporally weighted regression models. Int. J. Geogr. Inf. Sci., 1–23 https://doi.org/10.1080/13658816.2021.1882681.

Hou, W., Gao, J., Wu, S., Dai, E., 2015. Interannual variations in growing-season NDVI and its correlation with climate variables in the southwestern karst region of China. Remote Sens. 7, 11105–11124. https://doi.org/10.3390/rs70911105.

Hu, Q., Woodruff, C., Mudrick, S.E., 1998. Interdecadal variations of annual precipitation in the Central United States. B. Am. Meteorol. Soc. 79, 221–230. https://doi.org/10.1175/1520-0477(1998)079<0221:IVOAPI>2.0.CO;2.

Hu, C., Griffis, T.J., Baker, J.M., Wood, J.D., Millet, D.B., Yu, Z., Lee, X., 2020. Modeling the sources and transport processes during extreme ammonia episodes in the US Corn Belt. J. Geophys. Res.-Atmos. 125, e2019JD031207. https://doi.org/10.1029/2019JD031207.

Hu, C., Griffis, T.J., Frie, A., Baker, J.M., Wood, J.D., Millet, D.B., Yu, Z., Yu, X., Czarnetzki, A.C., 2021. A multiyear constraint on ammonia emissions and deposition within the US corn belt. Geophys. Res. Lett. 48, e2020GL090865. https://doi.org/10.1029/2020GL090865.

Huang, B., Wu, B., Barry, M., 2010. Geographically and temporally weighted regression for modeling spatio-temporal variation in house prices. Int. J. Geogr. Inf. Sci. 24, 383–401. https://doi.org/10.1080/13658810802672469.

Hurvich, C.M., Simonoff, J.S., Tsai, C.L., 1998. Smoothing parameter selection in nonparametric regression using an improved Akaike information criterion. J. Roy. Stat. Soc. B. 60, 271–293. https://doi.org/10.1111/1467-9868.00125.

Karl, T.R., Knight, R.W., 1998. Secular trends of precipitation amount, frequency, and intensity in the United States. B. Am. Meteorol. Soc. 79, 231–242. https://doi.org/10.1175/1520-0477(1998)079<0231:STOPAF>2.0.CO;2.

Kim, S., 2015. ppcor: an R package for a fast calculation to semi-partial correlation coefficients. Commun. Stat. Appl. Meth. 22, 665–674. https://doi.org/10.5351/CSAM.2015.22.6.665.

Li, Y., Thompson, T.M., Damme, M.V., Chen, X., Benedict, K.B., Shao, Y., Day, D., Boris, A., Sullivan, A.P., Ham, J., 2017. Temporal and spatial variability of ammonia in urban and agricultural regions of northern Colorado, United States. Atmos. Chem. Phys. 17, 6197–6213. https://doi.org/10.5194/acp-17-6197-2017.

Ma, R., Zou, J., Han, Z., Yu, K., Wu, S., Li, Z., Liu, S., Niu, S., Horwath, W.R., Zhu-Barker, X., 2021. Global soil-derived ammonia emissions from agricultural nitrogen fertilizer application: a refinement based on regional and crop-specific emission factors. Glob. Chang. Biol. 27, 855–867. https://doi.org/10.1111/gcb.15437.

Marchetto, A., Rogora, M., Arisci, S., 2013. Trend analysis of atmospheric deposition data: a comparison of statistical approaches. Atmos. Environ. 64, 95–102. https://doi.org/10.1016/j.atmosenv.2012.08.020.

Misselbrook, T., Hunt, J., Perazzolo, F., Provolo, G., 2016. Greenhouse gas and ammonia emissions from slurry storage: impacts of temperature and potential mitigation through covering (pig slurry) or acidification (cattle slurry). J. Environ. Qual. 45, 1520–1530. https://doi.org/10.2134/jeq2015.12.0618.

Nair, A.A., Yu, F., Luo, G., 2019. Spatioseasonal variations of atmospheric ammonia concentrations over the United States: comprehensive model-observation comparison. J. Geophysical Res.-Atmos. 124, 6571–6582. https://doi.org/10.1029/2018JD030057.

Nemitz, E., Milford, C., Sutton, M.A., 2001. A two-layer canopy compensation point model for describing bi-directional biosphere-atmosphere exchange of ammonia. Q. J. R. Meteorol. Soc. 127, 815–833. https://doi.org/10.1002/qj.49712757306.

Qu, S., Hu, S., Li, W., Zhang, C., Li, Q., Wang, H., 2020. Temporal variation in the effects of impact factors on residential land prices. Appl. Geogr. 114, 102124. https://doi.org/10.1016/j.apgeog.2019.102124.

Shen, H., Chen, Y., Hu, Y., Ran, L., Lam, S.K., Pavur, G.K., Zhou, F., Pleim, J.E., Russell, A.G., 2020a. Intense warming will significantly increase cropland ammonia volatilization threatening food security and ecosystem health. One Earth 3, 126–134. https://doi.org/10.1016/j.oneear.2020.06.015.

Shen, X., Zhou, Y., Jin, S., Wang, D., 2020b. Spatiotemporal influence of land use and household properties on automobile travel demand. Transport. Res. D.-Tr. E. 84, 102359. https://doi.org/10.1016/j.trd.2020.102359.

Shephard, M., Cady-Pereira, K., Luo, M., Henze, D., Pinder, R., Walker, J., Rinsland, C., Bash, J., Zhu, L., Payne, V., 2011. TES ammonia retrieval strategy and global observations of the spatial and seasonal variability of ammonia. Atmos. Chem. Phys. 11, 10743–10763. https://doi.org/10.5194/acp-11-10743-2011.

Shephard, M.W., Dammers, E., Cady-Pereira, K.E., Kharol, S.K., Thompson, J., Gainariu-Matz, Y., Zhang, J., McLinden, C.A., Kovachik, A., Moran, M., 2020. Ammonia measurements from space with the Cross-track Infrared Sounder: characteristics and applications. Atmos. Chem. Phys. 20, 2277–2302. https://doi.org/10.5194/acp-20-2277-2020.

Sinha, E., Michalak, A.M., 2016. Precipitation dominates interannual variability of riverine nitrogen loading across the continental United States. Environ. Sci. Technol. 50, 12874–12884. https://doi.org/10.1021/acs.est.6b04455.

Stephen, K., Aneja, V.P., 2008. Trends in agricultural ammonia emissions and ammonium concentrations in precipitation over the southeast and Midwest United States. Atmos. Environ. 42, 3238–3252. https://doi.org/10.1016/j.atmosenv.2007.05.062.

Sutton, M.A., Reis, S., Riddick, S.N., Dragosits, U., Nemitz, E., Theobald, M.R., Tang, Y.S., Braban, C.F., Vieno, M., Dore, A.J., 2013. Towards a climate-dependent paradigm of ammonia emission and deposition. Philos. T. R. Soc. B. 368, 20130166. https://doi.org/10.1098/rstb.2013.0166.

Thornton, M.M., Thornton, P.E., Wei, Y., Mayer, B.W., Cook, R.B., Vose, R.S., 2016. Daymet: Monthly Climate Summaries on a 1-km grid for North America, Version 3. ORNL Distributed Active Archive Center https://doi.org/10.3334/ORNLDAAC/1345.

Tian, H., Xu, R., Canadell, J.G., Thompson, R.L., Winiwarter, W., Suntharalingam, P., Davidson, E.A., Ciais, P., Jackson, R.B., Janssens-Maenhout, G., Prather, M.J., Regnier, P., Pan, N., Pan, S., Peters, G.P., Shi, H., Tubiello, F.N., Zaehle, S., Zhou, F., Arneth, A., Battaglia, G., Berthet, S., Bopp, L., Bouwman, A.F., Buitenhuis, E.T., Chang, J., Chipperfield, M.P., Dangal, S.R.S., Dlugokencky, E., Elkins, J.W., Eyre, B.D., Fu, B., Hall, B., Ito, A., Joos, F., Krummel, P.B., Landolfi, A., Laruelle, G.G., Lauerwald, R., Li, W., Lienert, S., Maavara, T., MacLeod, M., Millet, D.B., Olin, S., Patra, P.K., Prinn, R.G., Raymond, P.A., Ruiz, D.J., van der Werf, G.R., Vuichard, N., Wang, J., Weiss, R.F., Wells, K.C., Wilson, C., Yang, J., Yao, Y., 2020. A comprehensive quantification of global nitrous oxide sources and sinks. Nature 586, 248–256. https://doi.org/10.1038/S41586-020-2780-0.

USDA-ERS, 2013. Fertilizer use and price. U.S. Department of Agriculture-Economic Research Servicehttps://www.ers.usda.gov/data-products/fertilizer-use-and-price.aspx.

Van Damme, M., Clarisse, L., Whitburn, S., Hadji-Lazaro, J., Hurtmans, D., Clerbaux, C., Coheur, P.-F., 2018. Industrial and agricultural ammonia point sources exposed. Nature 564, 99–103. https://doi.org/10.1038/S41586-018-0747-1.

Van Damme, M., Clarisse, L., Franco, B., Sutton, M.A., Erisman, J.W., Kruit, R.W., van Zanten, M., Whitburn, S., Hadji-Lazaro, J., Hurtmans, D., 2020. Global, regional and national trends of atmospheric ammonia derived from a decadal (2008-2018) satellite record. Environ. Res. Lett. https://doi.org/10.1088/1748-9326/abd5e0.

Wang, R., Guo, X., Pan, D., Kelly, J.T., Bash, J.O., Sun, K., Paulot, F., Clarisse, L., Van Damme, M., Whitburn, S., 2021. Monthly patterns of ammonia over the contiguous United States at 2 km resolution. Geophys. Res. Lett. 48, e2020GL090579. https://doi.org/10.1029/2020GL090579.

Warner, J.X., Wei, Z., Strow, L.L., Dickerson, R.R., Nowak, J.B., 2016. The global tropospheric ammonia distribution as seen in the 13-year AIRS measurement record. Atmos. Chem. Phys. 16, 5467–5479. https://doi.org/10.5194/acp-16-5467-2016.

Warner, J., Dickerson, R., Wei, Z., Strow, L.L., Wang, Y., Liang, Q., 2017. Increased atmospheric ammonia over the world's major agricultural areas detected from space. Geophys. Res. Lett. 44, 2875–2884. https://doi.org/10.1002/2016GL072305.

Wu, C., Ren, F., Hu, W., Du, Q., 2019. Multiscale geographically and temporally weighted regression: exploring the spatiotemporal determinants of housing prices. Int. J. Geogr. Inf. Sci. 33, 489–511. https://doi.org/10.1080/13658816.2018.1545158.
Xu, R., Pan, S., Chen, J., Chen, G., Yang, J., Dangal, S., Shepard, J., Tian, H., 2018. Half-century ammonia emissions from agricultural systems in southern Asia: magnitude, spatio-temporal patterns, and implications for human health. GeoHealth 2, 40–53. https://doi.org/10.1002/2017GH000098.
Xu, R., Tian, H., Pan, S., Prior, S.A., Feng, Y., Batchelor, W.D., Chen, J., Yang, J., 2019. Global ammonia emissions from synthetic nitrogen fertilizer applications in agricultural systems: empirical and process-based estimates and uncertainty. Glob. Chang. Biol. 25, 314–326. https://doi.org/10.1111/gcb.14499.
Yu, F., Nair, A.A., Luo, G., 2018. Long-term trend of gaseous ammonia over the United States: modeling and comparison with observations. J. Geophys. Res.-Atmos. 123, 8315–8325. https://doi.org/10.1029/2018JD028412.
Zhan, X., Adalibieke, W., Cui, X., Winiwarter, W., Reis, S., Zhang, L., Bai, Z., Wang, Q., Huang, W., Zhou, F., 2021. Improved estimates of ammonia emissions from global croplands. Environ. Sci. Technol. 55, 1329–1338. https://doi.org/10.1021/acs.est.0c05149.